arXiv:1411.0070v2 [cond-mat.supr-con] 11 Mar 2015

Glide-Plane Symmetry and Superconducting Gap Structure of Iron-Based Superconductors

Y. Wang,[1,2,3] T. Berlijn,[1,4] P. J. Hirschfeld,[3] D. J. Scalapino,[5] and T. A. Maier[1,4]

[1] *Center for Nanophase Materials Sciences, Oak Ridge National Laboratory, Oak Ridge, Tennessee 37831, USA*
[2] *Department of Physics and Astronomy, University of Tennessee, Knoxville, Tennessee 37996, USA*
[3] *Department of Physics, University of Florida, Gainesville, Florida 32611, USA*
[4] *Computer Science and Mathematics Division, Oak Ridge National Laboratory, Oak Ridge, Tennessee 37831, USA*
[5] *Department of Physics, University of California, Santa Barbara, California 93106-9530, USA*

We consider the effect of glide-plane symmetry of the Fe-pnictogen/chalcogen layer in Fe-based superconductors on pairing in spin fluctuation models. Recent theories have proposed that so-called η-pairing states with nonzero total momentum can be realized and possess exotic properties such as odd parity spin singlet symmetry and time-reversal symmetry breaking. Here we show that η pairing is inevitable when there is orbital weight at the Fermi level from orbitals with even and odd mirror reflection symmetry in z; however, by explicit calculation, we conclude that the gap function that appears in observable quantities is identical to that found in earlier, 1 Fe per unit cell pseudocrystal momentum calculations.

PACS numbers: 74.20.Rp, 74.70.Xa, 74.20.Mn, 74.20.Pq

The common element in the crystal structure of all Fe-based superconductors is a two-dimensional plane of Fe atoms on a square lattice with pnictogen/chalcogen atoms sitting in alternating positions below or above the center of each square [1–4]. The alternating buckling of pnictogen/chalcogen atoms results in a unit cell with two inequivalent Fe atoms. A model that takes into account all Fe d orbitals therefore has ten orbitals (five d-orbitals per Fe). In spite of this, most theoretical calculations (e.g., Refs. 5 and 6 and many others) have been carried out using a five-orbital model for an "unfolded" Brillouin zone (BZ) of the 1 Fe unit cell, which appears to miss the effects of the out-of-plane pnictogen/chalcogen degrees of freedom on the band structure. In particular, an important question has been raised regarding whether these five-orbital calculations can correctly determine the superconducting properties such as the gap structure, given the large nonperturbative effects of the pnictogen/chalcogen potential that appear to be neglected in these studies. In addition there are questions regarding the possibility of odd parity spin singlet [7–9] and time-reversal breaking [10] associated with the so-called η pairing [7–11].

To better understand this issue, we review the implications of the glide-plane symmetry of a single Fe-pnictogen/chalcogen plane, as has been discussed before by various authors [12–17]: While the 1 Fe lattice does not have translational symmetry since the two sublattices A and B made up, respectively, of the two different Fe atoms are inequivalent, it is symmetric under the glide-plane symmetry operation $P_z = T_r\sigma_z$, i.e., a one unit translation along the x- or y-direction T_r combined with a reflection σ_z along z. As a consequence, the diagonal intrasublattice hopping between d orbitals that are even under P_z (xy, x^2-y^2, $3z^2-r^2$) and orbitals that are odd (xz, yz) changes sign between the A and B sublattice. When transformed to the physical 1 Fe crystal momentum $\mathbf{k}$ space, this leads to a mixing between momenta $\mathbf{k}$ and $\mathbf{k}+\mathbf{Q}$ with $\mathbf{Q}=(\pi,\pi)$ of the type $\sum_{\mathbf{k},\sigma}\left[t^{xz,xy}(\mathbf{k})c^\dagger_{xz,\sigma,\mathbf{k}+\mathbf{Q}}c_{xy,\sigma,\mathbf{k}}+\text{H.c.}\right]$, and other similar terms between even and odd (with respect to P_z) orbitals. Because of this, there are off-diagonal propagators involving even and odd orbitals with momenta $\mathbf{k}$ and $\mathbf{k}+\mathbf{Q}$. This has important consequences with respect to the pairing: in addition to the standard zero center of mass momentum pairs $\langle c_{\ell_1,\uparrow,\mathbf{k}}c_{\ell_2,\downarrow,-\mathbf{k}}\rangle$ for ℓ_1,ℓ_2 either both even or both odd orbitals, there are also nonzero total momentum η pairs $\langle c_{\ell_1,\uparrow,\mathbf{k}}c_{\ell_2,\downarrow,-\mathbf{k}+\mathbf{Q}}\rangle$ for ℓ_1 even, ℓ_2 odd or vice versa [10].

However, this mixing is absent if one uses the eigenvalues of P_z, i.e., the pseudocrystal momentum $\tilde{\mathbf{k}}$, to classify the states [12–14]. This basically corresponds to shifting the momentum of either the even or the odd orbitals by $\mathbf{Q}$. Here we choose the shift in the even orbitals so that states defined in the pseudocrystal momentum $\tilde{\mathbf{k}}$ are related to the states defined with the physical crystal momentum $\mathbf{k}$ through

$$\tilde{c}_{\ell,\sigma,\tilde{\mathbf{k}}}=\begin{cases}c_{\ell,\sigma,\mathbf{k}}, & \text{if } \ell \text{ odd},\\ c_{\ell,\sigma,\mathbf{k}+\mathbf{Q}}, & \text{if } \ell \text{ even}.\end{cases} \tag{1}$$

The Hamiltonian is diagonal in $\tilde{\mathbf{k}}$ and, as we will discuss, the usual five-orbital calculations, when performed in this space, automatically take into account the additional terms stemming from the mixing between $\mathbf{k}$ and $\mathbf{k}+\mathbf{Q}$ in the physical 1 Fe crystal momentum $\mathbf{k}$ space. Here η pairing is implicitly included since pairs like $\langle\tilde{c}_{xy,\uparrow,\tilde{\mathbf{k}}}\tilde{c}_{xz,\downarrow,-\tilde{\mathbf{k}}}\rangle$ in $\tilde{\mathbf{k}}$ space transform to $\langle c_{xy,\uparrow,\mathbf{k}}c_{xz,\downarrow,-\mathbf{k}+\mathbf{Q}}\rangle$ in $\mathbf{k}$ space as indicated in Fig. 1(c). Here we study the parity properties of these terms, the way in which they combine with normal (zero center of mass momentum) pairing states, and their implications for the gap structure in the

physical crystal momentum $\mathbf{k}$ space. We calculate the one-particle spectral function in the proper crystal momentum space and show that the energy gaps deduced from spectral function leading edges correspond to those calculated in the 1 Fe zone, although the quasiparticle weights are strongly renormalized. We conclude that, as usual, an even frequency gap for a singlet pair has even parity in the band basis and there is no time-reversal symmetry breaking as a result of η pairing.

To this end, we use the 2D five-orbital tight-binding model for LaOFeAs introduced in Graser *et al.* [6]. This model was obtained from a Wannier transformation of a local density approximation band structure calculation of this compound with a 2 Fe ten-orbital model and performing a gauge transformation corresponding to a π-phase shift of the even orbitals on the B sublattice, which in momentum space corresponds to a transformation to pseudocrystal $\tilde{\mathbf{k}}$ momentum. The Fermi surface of this model in the 1 Fe pseudocrystal momentum $\tilde{\mathbf{k}}$ space is shown in Fig. 1(a), with the dominant orbital weights indicated by the coloring. The corresponding Fermi surface in physical crystal momentum $\mathbf{k}$-space is plotted in Fig. 1(c). According to Eq. (1), it is obtained by shifting the even orbital contribution by $\mathbf{Q}$. The size of the points indicates the sum of the orbital weights.

This model is then supplemented with the usual Hubbard (intraorbital U and interorbital U') and Hund (Hund's rule coupling J and pair hopping J') interactions. Here we assume spin rotational invariance so that $U' = U - 2J$ and $J' = J$; set $U = 1.3\,\mathrm{eV}$ and $J = 0.2\,\mathrm{eV}$, and take $\langle n\rangle = 5.95$. We then use a random-phase approximation to calculate the pairing interaction $\Gamma_{\ell_1\ell_2\ell_3\ell_4}(\tilde{\mathbf{k}},\tilde{\mathbf{k}}')$ which represents the particle-particle scattering of electrons in orbitals ℓ_1,ℓ_4 with momenta $(\tilde{\mathbf{k}},-\tilde{\mathbf{k}})$ to electrons in orbitals ℓ_2,ℓ_3 with momenta $(\tilde{\mathbf{k}}',-\tilde{\mathbf{k}}')$. The pairing strengths λ_α for various pairing channels α are then given as the eigenvalues of

$$-\sum_j \oint_{C_j} \frac{d\tilde{\mathbf{k}}'_\parallel}{(2\pi)^2 v_F(\tilde{\mathbf{k}}'_\parallel)}\Gamma_{ij}(\tilde{\mathbf{k}},\tilde{\mathbf{k}}')g_\alpha(\tilde{\mathbf{k}}') = \lambda_\alpha g_\alpha(\tilde{\mathbf{k}})\,. \quad (2)$$

Here, $\Gamma_{ij}(\tilde{\mathbf{k}},\tilde{\mathbf{k}}')$ represents the irreducible vertex for the scattering of a pair of electrons $(\tilde{\mathbf{k}}\uparrow,-\tilde{\mathbf{k}}\downarrow)$ on Fermi pocket C_i to $(\tilde{\mathbf{k}}'\uparrow,-\tilde{\mathbf{k}}'\downarrow)$ on pocket C_j. It is obtained from $\Gamma_{\ell_1\ell_2\ell_3\ell_4}(\tilde{\mathbf{k}},\tilde{\mathbf{k}}')$ as

$$\Gamma_{ij}(\tilde{\mathbf{k}},\tilde{\mathbf{k}}') = \sum_{\ell_1,\ell_2,\ell_3,\ell_4} \tilde{a}^{\ell_1^*}_{\nu,\tilde{\mathbf{k}}}\tilde{a}^{\ell_4^*}_{\nu,-\tilde{\mathbf{k}}}\Gamma_{\ell_1\ell_2\ell_3\ell_4}(\tilde{\mathbf{k}},\tilde{\mathbf{k}}') \times\tilde{a}^{\ell_2}_{\mu,\tilde{\mathbf{k}}'}\tilde{a}^{\ell_3}_{\mu,-\tilde{\mathbf{k}}'}\,, \quad (3)$$

where the matrix elements $\tilde{a}^{\ell}_{\nu,\tilde{\mathbf{k}}} = \langle\widetilde{\ell\mathbf{k}}|\widetilde{\nu\mathbf{k}}\rangle$ transform the orbital basis to the band representation in pseudocrystal momentum space. The momenta $\tilde{\mathbf{k}}$ and $\tilde{\mathbf{k}}'$ in Eq. (3) are restricted to the Fermi surface and $v_F(\tilde{\mathbf{k}}'_\parallel)$ is the Fermi velocity. The eigenfunction $g_\alpha(\tilde{\mathbf{k}})$ for the largest eigenvalue determines the leading pairing instability and provides an approximate form for the superconducting gap $\tilde{\Delta}(\tilde{\mathbf{k}}) \propto g_\alpha(\tilde{\mathbf{k}})$. The structure of the leading gap function $g_\alpha(\tilde{\mathbf{k}})$ with $s_\pm$-wave symmetry on the Fermi surface is shown in Fig. 1(b).

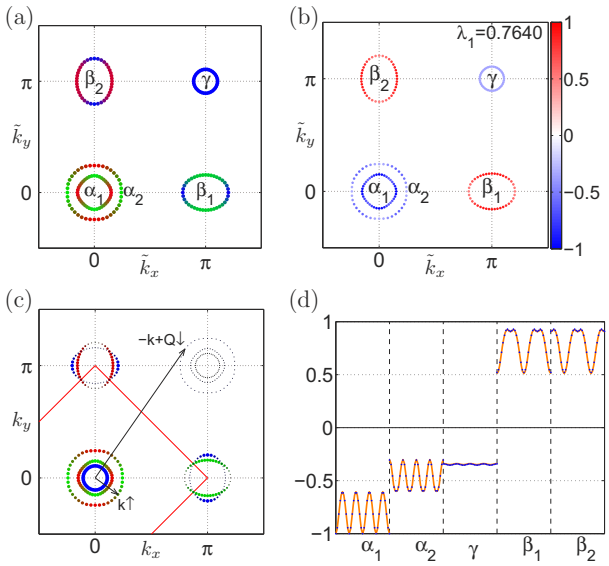

FIG. 1. (color online). (a) Fermi surfaces and (b) the leading gap function for the five-orbital model in the zone of the pseudocrystal momentum $\tilde{\mathbf{k}}$. The Fermi surface is colored to show the dominant orbital weight [d_{xz} red (gray), d_{yz} green (light gray), d_{xy} blue (dark gray)]. (c) The unfolded Fermi surface in the physical crystal momentum $\mathbf{k}$-space. The size of the dots is proportional to the sum of the orbital weights of the spectral function and the color shows the dominant orbital weight. The red line denotes the boundary of the 2 Fe per unit cell Brillouin zone. An "η" pair $(\mathbf{k}\uparrow,-\mathbf{k}+\mathbf{Q}\downarrow)$ is shown. (d) Comparison of the angle dependence of the leading gap function calculated from the five-orbital model (orange line) and the ten-orbital model (blue dots) on the various Fermi pockets. Here we denote the two crossed electron pockets in the ten-orbital model at the X point as β_1 and β'_1 and at the Y point β_2 and β'_2. The gaps along the $\beta'_{1,2}$ pockets are not plotted since $\beta'_1 = \beta_2$ and $\beta'_2 = \beta_1$ by symmetry.

We have also calculated the leading gap function and the eigenvalue in the original ten-orbital model, from which the five-orbital model was derived through a gauge transformation, as discussed above. We obtain the same leading eigenvalue $\lambda = 0.76$ in the ten-orbital as in the five-orbital model, and Fig. 1(d) shows that the gap function obtained in the ten-orbital model is identical to what is obtained in the five-orbital model. From this it is clear that calculations performed in the 1 Fe five-orbital pseudocrystal momentum space indeed contain all information of the more complex ten-orbital calculation performed in the 2 Fe crystal momentum space.

As discussed above, this includes the information about η-pairing terms in the physical 1 Fe momentum $\mathbf{k}$ space. In order to analyze the structure of these terms,

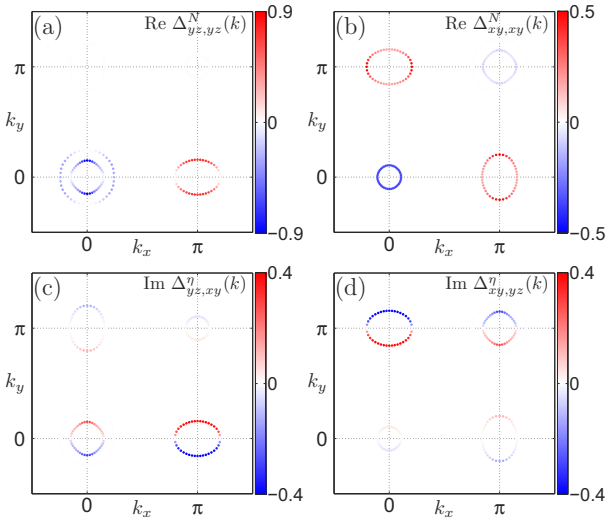

FIG. 2. (color online). Gap functions $\Delta_{\ell_1\ell_2}(\mathbf{k})$ in the orbital basis plotted on the Fermi surface in the physical momentum BZ. (a)–(b) When ℓ_1 and ℓ_2 have the same z-reflection symmetry, one has a normal $(\mathbf{k},-\mathbf{k})$ pairing and the gap function $\Delta^N_{\ell_1\ell_2}(\mathbf{k})$ is real and has even parity. (c)–(d) When ℓ_1 and ℓ_2 have different z-reflection symmetry, one has a $(\mathbf{k},-\mathbf{k}+\mathbf{Q})$ η pairing and $\Delta^\eta_{\ell_1\ell_2}(\mathbf{k})$ is purely imaginary and has odd parity.

we transform the gap function $\tilde{\Delta}_\nu(\tilde{\mathbf{k}})$ that we obtained in pseudocrystal momentum space to 1 Fe physical crystal momentum $\mathbf{k}$ space. To this end, we first transform $\tilde{\Delta}_\nu(\tilde{\mathbf{k}})$ from band to orbital space and then to $\mathbf{k}$ space. This gives normal pairing terms with zero center of mass momentum,

$$\langle c_{\ell_1\uparrow,\mathbf{k}} c_{\ell_2\downarrow,-\mathbf{k}} - c_{\ell_1\downarrow,\mathbf{k}} c_{\ell_2\uparrow,-\mathbf{k}}\rangle \propto \Delta^N_{\ell_1\ell_2}(\mathbf{k}) = \begin{cases} \tilde{a}^{\ell_1}_{\nu,\mathbf{k}}\tilde{a}^{\ell_2}_{\nu,-\mathbf{k}}\tilde{\Delta}_\nu(\mathbf{k}), & \ell_1,\ell_2 \text{ odd}, \\ \tilde{a}^{\ell_1}_{\nu,\mathbf{k}-\mathbf{Q}}\tilde{a}^{\ell_2}_{\nu,-\mathbf{k}+\mathbf{Q}}\tilde{\Delta}_\nu(\mathbf{k}-\mathbf{Q}), & \ell_1,\ell_2 \text{ even}, \\ 0, & \text{otherwise}, \end{cases} \tag{4}$$

and η-pairing terms with center of mass momentum $\mathbf{Q}$,

$$\langle c_{\ell_1\uparrow,\mathbf{k}} c_{\ell_2\downarrow,-\mathbf{k}+\mathbf{Q}} - c_{\ell_1\downarrow,\mathbf{k}} c_{\ell_2\uparrow,-\mathbf{k}+\mathbf{Q}}\rangle \propto \Delta^\eta_{\ell_1\ell_2}(\mathbf{k}) = \begin{cases} \tilde{a}^{\ell_1}_{\nu,\mathbf{k}}\tilde{a}^{\ell_2}_{\nu,-\mathbf{k}}\tilde{\Delta}_\nu(\mathbf{k}), & \ell_1 \text{ odd}, \ell_2 \text{ even}, \\ \tilde{a}^{\ell_1}_{\nu,\mathbf{k}-\mathbf{Q}}\tilde{a}^{\ell_2}_{\nu,-\mathbf{k}+\mathbf{Q}}\tilde{\Delta}_\nu(\mathbf{k}-\mathbf{Q}), & \ell_1 \text{ even}, \ell_2 \text{ odd}, \\ 0, & \text{otherwise}. \end{cases} \tag{5}$$

Here and in the following we have replaced $\tilde{\mathbf{k}}$ by $\mathbf{k}$ for odd and $\mathbf{k}+\mathbf{Q}$ for even orbitals ℓ, as noted in Eq. (1). For a given Fermi momentum $\mathbf{k}$, ν labels the band that crosses the Fermi energy at $\mathbf{k}$.

Figure 2 shows the gap functions $\Delta_{\ell_1\ell_2}(\mathbf{k})$ for four different combinations of orbitals ℓ_1 and ℓ_2. In Figs. 2(a) and 2(b), one sees that when ℓ_1 and ℓ_2 have the same z-reflection symmetry, one has a normal $(\mathbf{k},-\mathbf{k})$ pairing and the gap function $\Delta^N_{\ell_1\ell_2}(\mathbf{k})$ is real and has even parity, i.e., $\Delta^N_{\ell_1\ell_2}(-\mathbf{k}) = \Delta^N_{\ell_1\ell_2}(\mathbf{k})$. In contrast, when ℓ_1 and ℓ_2 have different z-reflection symmetry, one has a $(\mathbf{k},-\mathbf{k}+\mathbf{Q})$ η pairing. In this case, $\Delta^\eta_{\ell_1\ell_2}(\mathbf{k})$ is purely imaginary and has odd parity, i.e., $\Delta^\eta_{\ell_1\ell_2}(-\mathbf{k}) = -\Delta^\eta_{\ell_1\ell_2}(\mathbf{k})$. Note that these gaps have the same behavior under mirror reflections as the orbitally resolved gaps of Casula and Sorella [15]. Here we stress that the odd parity and the imaginary nature of these terms in orbital space arises entirely from the product of matrix elements $\tilde{a}^{\ell_1}_{\nu,\mathbf{k}}\tilde{a}^{\ell_2}_{\nu,-\mathbf{k}}$ and, therefore, is merely a reflection of the glide-plane symmetry of the Fe-pnictogen/chalcogen plane. It does not reflect any exotic behavior of the pairing interaction. We also point out that time-reversal symmetry requires that $\Delta_{\ell_1\ell_2}(\mathbf{k}) = \Delta^*_{\ell_1\ell_2}(-\mathbf{k})$ for both the normal and η gaps in Eqs. (4) and (5), respectively. Because the normal gap $\Delta^N_{\ell_1\ell_2}(\mathbf{k})$ has even parity and is purely real, it satisfies time-reversal symmetry, as does the odd parity, purely imaginary η-pairing gap $\Delta^\eta_{\ell_1\ell_2}(\mathbf{k})$. Both normal and η-pairing terms, however, coexist in orbital space and contribute to the pairing condensate.

This raises the question of how these two terms combine, given their opposite parity. To study this, we transform the gap back to band representation in physical crystal momentum $\mathbf{k}$ space and obtain, for the normal pairing,

$$\Delta^N_\nu(\mathbf{k}) = \Delta^N_{\text{odd}}(\mathbf{k}) + \Delta^N_{\text{even}}(\mathbf{k}), \tag{6}$$

where

$$\Delta^N_{\text{odd}}(\mathbf{k}) = \sum_{\ell_1,\ell_2\ \text{odd}} \tilde{a}^{\ell_1^*}_{\nu,\mathbf{k}}\tilde{a}^{\ell_2^*}_{\nu,-\mathbf{k}}\Delta^N_{\ell_1\ell_2}(\mathbf{k}), \tag{7a}$$

$$\Delta^N_{\text{even}}(\mathbf{k}) = \sum_{\ell_1,\ell_2\ \text{even}} \tilde{a}^{\ell_1^*}_{\nu,\mathbf{k}-\mathbf{Q}}\tilde{a}^{\ell_2^*}_{\nu,-\mathbf{k}+\mathbf{Q}}\Delta^N_{\ell_1\ell_2}(\mathbf{k}). \tag{7b}$$

Similarly, we obtain for the η-pairing terms,

$$\Delta^\eta_\nu(\mathbf{k}) = \Delta^\eta_{\text{odd-even}}(\mathbf{k}) + \Delta^\eta_{\text{even-odd}}(\mathbf{k}), \tag{8}$$

where

$$\Delta^\eta_{\text{odd-even}}(\mathbf{k}) = \sum_{\ell_1\ \text{odd},\ell_2\ \text{even}} \tilde{a}^{\ell_1^*}_{\nu,\mathbf{k}}\tilde{a}^{\ell_2^*}_{\nu,-\mathbf{k}}\Delta^\eta_{\ell_1\ell_2}(\mathbf{k}), \tag{9a}$$

$$\Delta^\eta_{\text{even-odd}}(\mathbf{k}) = \sum_{\ell_1\ \text{even},\ell_2\ \text{odd}} \tilde{a}^{\ell_1^*}_{\nu,\mathbf{k}-\mathbf{Q}}\tilde{a}^{\ell_2^*}_{\nu,-\mathbf{k}+\mathbf{Q}}\Delta^\eta_{\ell_1\ell_2}(\mathbf{k}). \tag{9b}$$

Here we have used the fact that the matrix elements $a^\ell_{\nu,\mathbf{k}}$, which provide the transformation from the orbital to the band representation in physical crystal momentum $\mathbf{k}$ space, are given by the matrix elements in pseudocrystal momentum space, $\tilde{a}^\ell_{\nu,\mathbf{k}}$ for ℓ denoting an odd orbital and $\tilde{a}^\ell_{\nu,\mathbf{k}-\mathbf{Q}}$ for ℓ denoting an even orbital.

Then, using Eqs. (4) and (5) one can show that the gap function $\tilde{\Delta}_\nu(\mathbf{k})$ calculated in the five-orbital model in the pseudocrystal momentum representation splits into normal and η-pairing terms in the physical crystal momentum space, i.e.,

$$\tilde{\Delta}_\nu(\mathbf{k}) = \Delta^N_{\text{odd}}(\mathbf{k}) + \Delta^N_{\text{even}}(\mathbf{k}+\mathbf{Q}) + \Delta^\eta_{\text{odd-even}}(\mathbf{k}) + \Delta^\eta_{\text{even-odd}}(\mathbf{k}+\mathbf{Q}). \tag{10}$$

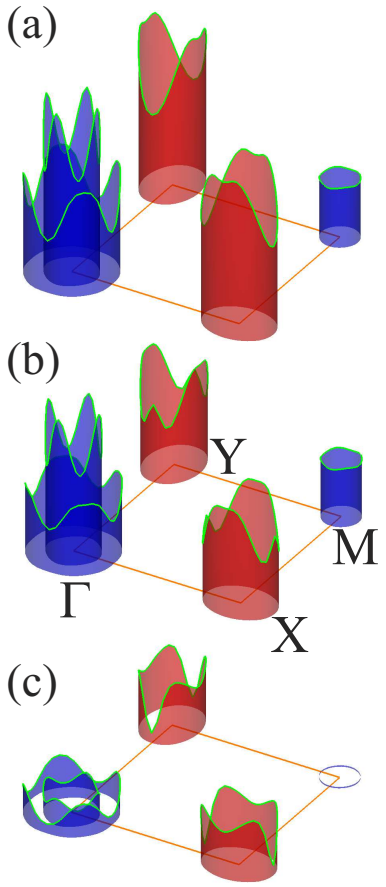

FIG. 3. (color online). (a) The leading gap function $\tilde{\Delta}(\tilde{\mathbf{k}})$ in the band representation calculated in the five-orbital model in pseudocrystal momentum space [red = positive (gap along pockets at X and Y points), blue = negative (gap along pockets at Γ and M points)]. When transformed to physical crystal momentum $\mathbf{k}$ space, the gap splits into the normal even-even and odd-odd contributions $\Delta^N_{\rm odd}(\mathbf{k})+\Delta^N_{\rm even}(\mathbf{k}+\mathbf{Q})$ plotted in (b) and the even-odd and odd-even η contributions $\Delta^\eta_{\text{odd-even}}(\mathbf{k})+\Delta^\eta_{\text{even-odd}}(\mathbf{k}+\mathbf{Q})$ shown in (c). In the band representation, all contributions have even parity.

Note that the even terms have their momentum shifted by $\mathbf{Q}$, so they appear on the same Fermi pockets as the odd terms. Figure 3 shows a graphical representation of this relation by plotting a 3D representation of $\tilde{\Delta}_\nu(\mathbf{k})$ in the top panel, its normal contribution $\Delta^N_{\rm odd}(\mathbf{k})+\Delta^N_{\rm even}(\mathbf{k}+\mathbf{Q})$ in the middle panel, and its η contribution $\Delta^\eta_{\text{odd-even}}(\mathbf{k})+\Delta^\eta_{\text{even-odd}}(\mathbf{k}+\mathbf{Q})$ in the bottom panel. One sees that after the transformation to band representation, the η-pairing term has even parity (and is real), just like the normal pairing contribution. This results from the combination of the product of matrix elements $\tilde{a}^{\ell_1^*}_{\nu,\mathbf{k}}\tilde{a}^{\ell_2^*}_{\nu,-\mathbf{k}}$, which has odd parity and is purely imaginary, with the odd parity and imaginary $\Delta^\eta_{\ell_1\ell_2}(\mathbf{k})$ for odd-even combinations of ℓ_1 and ℓ_2. Thus, as usual, an even frequency gap in the band basis has even parity for a singlet pair. From Eqs. (4)–(9) it is straightforward to show that the normal and η contributions to the gap have the same sign and share the same nodal structure in the case of a nodal gap [18]. Thus, while the η contribution is significant in the amplitude of the total gap, it does not affect its sign and nodal structure and therefore does not qualitatively alter the low temperature thermodynamic properties. This is discussed in more detail in the Supplemental Material [19].

Finally, we calculate the spectral function

$$A(\mathbf{k},\omega)=\sum_{\ell,\nu}|\langle\ell\mathbf{k}|\widetilde{\nu\mathbf{k}}\rangle|^2\tilde{A}_\nu(\tilde{\mathbf{k}},\omega)$$

as measured in angle-resolved photoemission spectroscopy (ARPES) experiments in the proper 1 Fe crystal momentum $\mathbf{k}$ space. Here, $\tilde{A}_\nu(\tilde{\mathbf{k}},\omega)=u^2_\nu(\tilde{\mathbf{k}})\delta(\omega-E_\nu(\tilde{\mathbf{k}}))+v^2_\nu(\tilde{\mathbf{k}})\delta(\omega+E_\nu(\tilde{\mathbf{k}}))$ is the BCS spectral function in the pseudocrystal momentum space with $E_\nu(\tilde{\mathbf{k}})=\sqrt{\epsilon^2_\nu(\tilde{\mathbf{k}})+\tilde{\Delta}^2_\nu(\tilde{\mathbf{k}})}$ and the BCS coherence factors $u^2_\nu(\tilde{\mathbf{k}})=[1+\epsilon_\nu(\tilde{\mathbf{k}})/E_\nu(\tilde{\mathbf{k}})]/2$ and $v^2_\nu(\tilde{\mathbf{k}})=1-u^2_\nu(\tilde{\mathbf{k}})$. Realizing that

$$\langle\ell\mathbf{k}|\widetilde{\nu\mathbf{k}}\rangle=\begin{cases}\tilde{a}^\ell_{\nu,\mathbf{k}}\delta_{\mathbf{k},\tilde{\mathbf{k}}}, & \ell \text{ odd},\\ \tilde{a}^\ell_{\nu,\mathbf{k}-\mathbf{Q}}\delta_{\mathbf{k}-\mathbf{Q},\tilde{\mathbf{k}}}, & \ell \text{ even},\end{cases}\tag{11}$$

one arrives at

$$A(\mathbf{k},\omega)=\sum_\nu\Bigg[\sum_{\ell\,\text{odd}}|\tilde{a}^\ell_{\nu,\mathbf{k}}|^2\tilde{A}_\nu(\mathbf{k},\omega)+\sum_{\ell\,\text{even}}|\tilde{a}^\ell_{\nu,\mathbf{k}-\mathbf{Q}}|^2\tilde{A}_\nu(\mathbf{k}-\mathbf{Q},\omega)\Bigg].\tag{12}$$

Thus, the superconducting gap that enters $A(\mathbf{k},\omega)$ as measured in ARPES experiments is given by the gap function $\tilde{\Delta}_\nu(\tilde{\mathbf{k}})$ calculated in the five-orbital 1 Fe zone in pseudocrystal momentum space and no further transformation is necessary. $\tilde{\Delta}_\nu(\tilde{\mathbf{k}})$ implicitly encodes the strong symmetry breaking potential associated with the pnictogen/chalcogen atom. The gap $\tilde{\Delta}_\nu(\tilde{\mathbf{k}})$ entering the first $\ell=$ "odd" term in Eq. (12) is shown in Fig. 3(a) while the gap entering the second $\ell=$ "even" contribution which appears on the "shadow" pockets is obtained by shifting the gap by $\mathbf{Q}$. As in the normal state [20–24], the spectral weight in the superconducting state associated with each contribution is modulated by the orbital weights $|\tilde{a}^\ell_{\nu,\mathbf{k}}|^2$ and $|\tilde{a}^\ell_{\nu,\mathbf{k}-\mathbf{Q}}|^2$, respectively, and this weight can differ substantially between the main and shadow pockets, as seen in Fig. 1(c). The spectral functions for both the normal and the superconducting states are discussed in more detail and shown in the Supplemental Material [19].

To summarize, we have carried out microscopic calculations of the superconducting gap structure in 1 Fe and 2 Fe per unit cell models and shown that η pairing is an important ingredient in the superconducting condensate. We have demonstrated that it contributes with

the usual even parity symmetry in band space and that time-reversal symmetry is preserved, in contrast to recent proposals in the literature. Finally we have shown that the gap function, which appears in observable quantities, is identical to that found in earlier, 1 Fe per unit cell pseudocrystal momentum calculations.

The authors acknowledge their useful discussions with A. Chubukov, M. Khodas, and W. Ku. P.J.H. and Y.W. were supported by Grant No. DOE DE-FG02-05ER46236, and T.B. was supported as a Wigner Fellow at the Oak Ridge National Laboratory. A portion of this research was conducted at the Center for Nanophase Materials Sciences, which is sponsored at Oak Ridge National Laboratory by the Scientific User Facilities Division, Office of Basic Energy Sciences, U.S. Department of Energy. This research was supported in part by Kavli Institute for Theoretical Physics under National Science Foundation Grant No. PHY11-25915.

[1] G. R. Stewart, Rev. Mod. Phys. **83**, 1589 (2011).
[2] H.-H. Wen and S. Li, Annu. Rev. Condens. Matter Phys. **2**, 121 (2011).
[3] P. J. Hirschfeld, M. M. Korshunov, and I. I. Mazin, Rep. Prog. Phys. **74**, 124508 (2011).
[4] P. Dai, J. Hu, and E. Dagotto, Nat. Phys. **8**, 709 (2012).
[5] K. Kuroki, S. Onari, R. Arita, H. Usui, Y. Tanaka, H. Kontani, and H. Aoki, Phys. Rev. Lett. **101**, 087004 (2008).
[6] S. Graser, T. A. Maier, P. J. Hirschfeld, and D. J. Scalapino, New J. Phys. **11**, 025016 (2009).
[7] J. Hu and N. Hao, Phys. Rev. X **2**, 021009 (2012).
[8] J. Hu, Phys. Rev. X **3**, 031004 (2013).
[9] N. Hao and J. Hu, Phys. Rev. B **89**, 045144 (2014).
[10] C.-H. Lin, C.-P. Chou, W.-G. Yin, and W. Ku, Orbital-parity distinct superconducting pairing structures of Fe-based superconductors under glide symmetry, arXiv:1403.3687.
[11] M. Khodas and A. V. Chubukov, Phys. Rev. Lett. **108**, 247003 (2012).
[12] P. A. Lee and X.-G. Wen, Phys. Rev. B **78**, 144517 (2008).
[13] H. Eschrig and K. Koepernik, Phys. Rev. B **80**, 104503 (2009).
[14] O. K. Andersen and L. Boeri, Ann. Phys. **523**, 8 (2011).
[15] M. Casula and S. Sorella, Phys. Rev. B **88**, 155125 (2013).
[16] M. H. Fischer, New J. Phys. **15**, 073006 (2013).
[17] V. Cvetkovic and O. Vafek, Phys. Rev. B **88**, 134510 (2013).
[18] To be more precise, $\Delta^N_{\rm odd}(\mathbf{k})$ and $\Delta^\eta_{\text{odd-even}}(\mathbf{k})$ have the same sign as $\tilde{\Delta}(\mathbf{k})$, and $\Delta^N_{\rm even}(\mathbf{k})$ and $\Delta^\eta_{\text{even-odd}}(\mathbf{k})$ have the same sign as $\tilde{\Delta}(\mathbf{k}-\mathbf{Q})$.
[19] See Supplemental Material at [url] for the effects of the η contribution on the spectral function, the dependence of its magnitude on doping and the case of a nodal gap in much greater detail.
[20] W. Ku, T. Berlijn, and C.-C. Lee, Phys. Rev. Lett. **104**, 216401 (2010).
[21] W. Lv and P. Phillips, Phys. Rev. B **84**, 174512 (2011).
[22] C.-H. Lin, T. Berlijn, L. Wang, C.-C. Lee, W.-G. Yin, and W. Ku, Phys. Rev. Lett. **107**, 257001 (2011).
[23] V. Brouet, M. F. Jensen, P.-H. Lin, A. Taleb-Ibrahimi, P. Le Fèvre, F. Bertran, C.-H. Lin, W. Ku, A. Forget, and D. Colson, Phys. Rev. B **86**, 075123 (2012).
[24] S. Kong, D. Y. Liu, S. T. Cui, S. L. Ju, A. F. Wang, X. G. Luo, L. J. Zou, X. H. Chen, G. B. Zhang, and Z. Sun, Electronic structure in one-Fe Brillouin zone of iron-pnictide superconductor $CsFe_2As_2$, arXiv:1409.2300.

[SUPPLEMENTAL INFORMATION]

S1. SINGLE PARTICLE SPECTRAL FUNCTION

As discussed in the main text and according to Eq. (12), the spectral function $\tilde{A}(\mathbf{k},\omega)$ in pseudocrystal momentum space splits into two contributions when transformed to physical crystal momentum space $\mathbf{k}$, i.e.,

$$\tilde{A}(\mathbf{k},\omega) = A_{\rm odd}(\mathbf{k},\omega) + A_{\rm even}(\mathbf{k}+\mathbf{Q},\omega)\,, \tag{13}$$

with

$$A_{\rm odd}(\mathbf{k},\omega) = \sum_\nu \sum_{\ell\,\rm odd} |\tilde{a}^\ell_{\nu,\mathbf{k}}|^2 \tilde{A}_\nu(\mathbf{k},\omega)\,, \tag{14}$$

$$A_{\rm even}(\mathbf{k}+\mathbf{Q},\omega) = \sum_\nu \sum_{\ell\,\rm even} |\tilde{a}^\ell_{\nu,\mathbf{k}}|^2 \tilde{A}_\nu(\mathbf{k},\omega)\,. \tag{15}$$

The first contribution has purely odd orbital character and appears at the same momentum $\mathbf{k}$, while the second contribution has even orbital character and is shifted by $\mathbf{Q}=(\pi,\pi)$. Each contribution is weighted by orbital matrix elements. This is illustrated in Fig. S1 where we plot the normal state spectral function with $\omega=0$ on the Fermi surface. The odd-orbital contribution is depicted in panel (a), while the $\mathbf{Q}$ shifted even-orbital contribution is shown in (b).

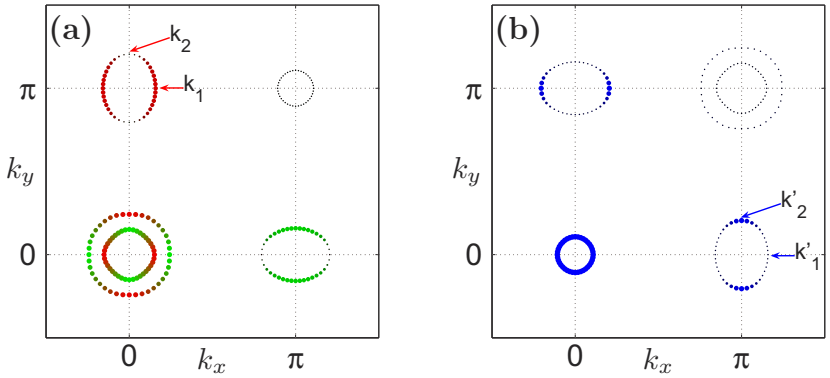

FIG. S1. The spectral function $A_{\rm odd}(\mathbf{k},\omega=0)$ (a) and $A_{\rm even}(\mathbf{k},\omega=0)$ (b) on the Fermi surface in physical crystal momentum space where the color shows the dominant orbital weight (d_{xz} red, d_{yz} green and d_{xy} blue). The size of the dots is proportional to $\sum_{\ell\,\rm odd}|\tilde{a}^{\ell}_{\nu,\mathbf{k}}|^2$ in (a) and $\sum_{\ell\,\rm even}|\tilde{a}^{\ell}_{\nu,\mathbf{k}-\mathbf{Q}}|^2$ in (b).

The frequency dependence of the spectral function near $\omega=0$ is plotted in Fig. S2 for momenta $\mathbf{k}_1$ and $\mathbf{k}_2$ on the "odd" parts of the Fermi surface, and for momenta $\mathbf{k}'_1$ and $\mathbf{k}'_2$ on the "even" parts. The four $\mathbf{k}$ points, $\mathbf{k}_{1,2}$ and $\mathbf{k}'_{1,2}$, are indicated in Fig. S1. These momenta are chosen so that $\mathbf{k}'_1=\mathbf{k}_1+\mathbf{Q}$ and $\mathbf{k}'_2=\mathbf{k}_2+\mathbf{Q}$ where $\mathbf{Q}=(\pi,-\pi)$. The green triangles depict the spectral function in pseudocrystal momentum space, $\tilde{A}(\mathbf{k}_{1,2},\omega)$, while the red and blue solid lines show the two contributions $A_{\rm odd}(\mathbf{k}_{1,2},\omega)$ and $A_{\rm even}(\mathbf{k}'_{1,2},\omega)$, respectively, in physical crystal momentum space. The spectral functions in the normal state are plotted in panels (a) and (d), while panels (b) and (e) are for the superconducting state, for which we have used the gap momentum structure shown in Fig. 1(d) with a maximum gap amplitude of 5 meV. The δ-functions entering the spectral functions are approximated by a Lorentzian, i.e., $\delta(\omega)\approx\zeta/[\pi(\omega^2+\zeta^2)]$ and we have used an artificial broadening $\zeta=0.3$ meV. From these plots one sees again how the spectral weights in the physical crystal momentum space at $\mathbf{k}_1$ and $\mathbf{k}'_1=\mathbf{k}_1+\mathbf{Q}$ add up to give the spectral weight in the pseudocrystal momentum space at $\mathbf{k}_1$. In the superconducting state, one sees that the leading edge gap in the "odd" part of the spectrum at momenta $\mathbf{k}_{1,2}$ is given by the gap $\tilde{\Delta}(\mathbf{k}_{1,2})$ calculated in pseudocrystal momentum space, while the gap in the "even" part of the spectrum at momenta $\mathbf{k}'_{1,2}$ is given by $\tilde{\Delta}(\mathbf{k}'_{1,2}-\mathbf{Q})=\tilde{\Delta}(\mathbf{k}_{1,2})$. To show the effect of the η gap on the spectral function, in Fig. S2 (c) and (f) we plot the spectral function at $\mathbf{k}_1$ ($\mathbf{k}'_1$) and $\mathbf{k}_2$ ($\mathbf{k}'_2$), respectively, for the superconducting state with the η contribution removed from the calculated gap function. As discussed in the main text, the normal and η contributions to the gap have the same sign as $\tilde{\Delta}(\mathbf{k})$. Because of the this, the gap in the spectral function would be reduced if the η contribution were removed.

S2. DOPING DEPENDENCE OF THE NORMAL AND η CONTRIBUTIONS TO THE GAP

As shown in the main text in Eq. (10), the gap function $\tilde{\Delta}_\nu(\mathbf{k})$ calculated in the five-orbital model in the pseudocrystal momentum representation splits into normal ($\Delta^N_{\rm odd}$ and $\Delta^N_{\rm even}$) and η-pairing terms ($\Delta^\eta_{\text{odd-even}}$ and $\Delta^\eta_{\text{even-odd}}$) in the physical crystal momentum space according to

$$\tilde{\Delta}_\nu(\mathbf{k})=\Delta^N_{\rm odd}(\mathbf{k})+\Delta^N_{\rm even}(\mathbf{k}+\mathbf{Q})+\Delta^\eta_{\text{odd-even}}(\mathbf{k})+\Delta^\eta_{\text{even-odd}}(\mathbf{k}+\mathbf{Q})\,. \tag{16}$$

Fig. S3 shows the ratios $R_{\rm odd}=\Delta^N_{\rm odd}(\mathbf{k})/\tilde{\Delta}_\nu(\mathbf{k})$, $R_{\rm even}=\Delta^N_{\rm even}(\mathbf{k}+\mathbf{Q})/\tilde{\Delta}_\nu(\mathbf{k})$ and $R_\eta=[\Delta^\eta_{\text{odd-even}}(\mathbf{k})+\Delta^\eta_{\text{even-odd}}(\mathbf{k}+\mathbf{Q})]/\tilde{\Delta}_\nu(\mathbf{k})$ for five different filling levels n. With increasing filling n, one sees that the relative contribution from the η pairing decreases on the hole pockets and increases along the $\pm\pi/4$ directions on the electron pockets. The overall change with doping is found to be rather weak and the η pairing remains significant for all doping levels.

S3. SUPERCONDUCTING GAP WITH NODES

The superconducting gap structure we have analyzed in the main text does not have nodes on the Fermi surface. Here we present the results of a calculation for different parameters (filling $n=5.95$, $U=1.3$ eV and $J=0$), for which we find an $s_\pm$ gap $\tilde{\Delta}(\mathbf{k})$ in pseudocrystal momentum space that has nodes on the electron pockets. Fig. S4 shows this gap structure plotted on the "odd" (a) and "even" (b) Fermi surface pockets, i.e., as it enters the spectral

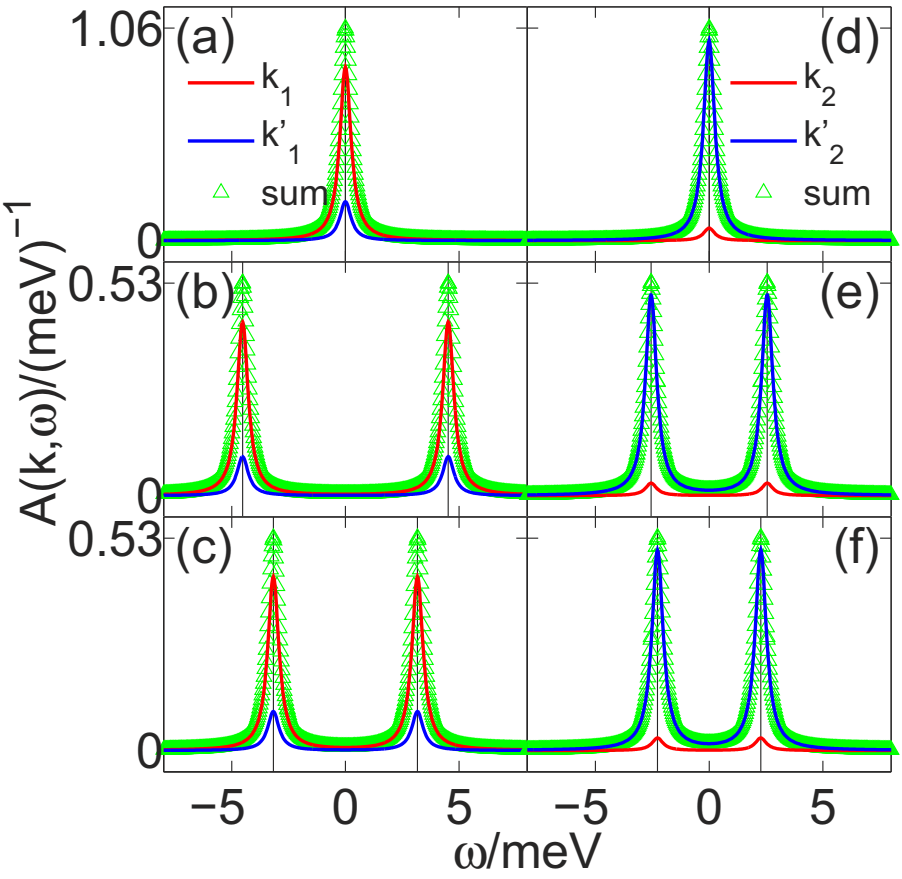

FIG. S2. Spectral function on the Fermi surface in physical crystal momentum space. Panels (a) and (d) are for the normal state, (b) and (e) for the superconducting state, and (c) and (f) for the superconducting state with the η contribution removed. Panels (a)–(c) are for momenta $\mathbf{k}_1$ and $\mathbf{k}'_1$ and (d)–(f) for $\mathbf{k}_2$ and $\mathbf{k}'_2$. The momenta are indicated on the Fermi surface in Fig. S1.

function. Since the gap is given by $\tilde{\Delta}(\mathbf{k})$ on the "odd" Fermi surfaces, but $\tilde{\Delta}(\mathbf{k}-\mathbf{Q})$ on the "even" pockets, the nodes on the electron pockets appear along different directions in the physical crystal momentum space. This is similar to what was discussed by C.-H. Lin *et al.* in Ref. 10.

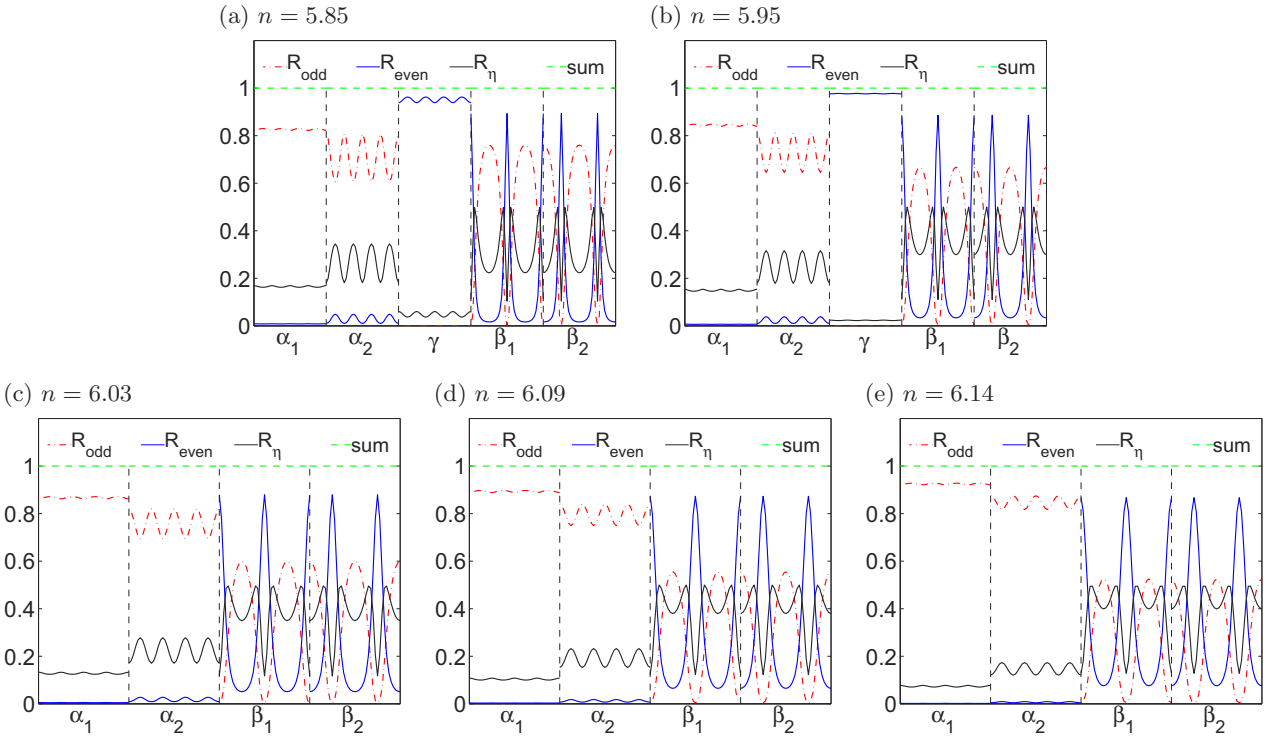

FIG. S3. (a)–(e): Ratios of $\Delta^N_{\rm odd}(\mathbf{k})/\tilde{\Delta}_\nu(\mathbf{k})$ (red dash-dotted line), $\Delta^N_{\rm even}(\mathbf{k}+\mathbf{Q})/\tilde{\Delta}_\nu(\mathbf{k})$ (blue solid line) and $[\Delta^\eta_{\text{odd-even}}(\mathbf{k}) + \Delta^\eta_{\text{even-odd}}(\mathbf{k}+\mathbf{Q})]/\tilde{\Delta}_\nu(\mathbf{k})$ (black solid line) for five different doping levels. Here $\mathbf{k}$ is along each Fermi pocket starting from $+k_x$ direction. Top row: hole doping with γ pocket. Bottom row: electron doping without γ pocket.

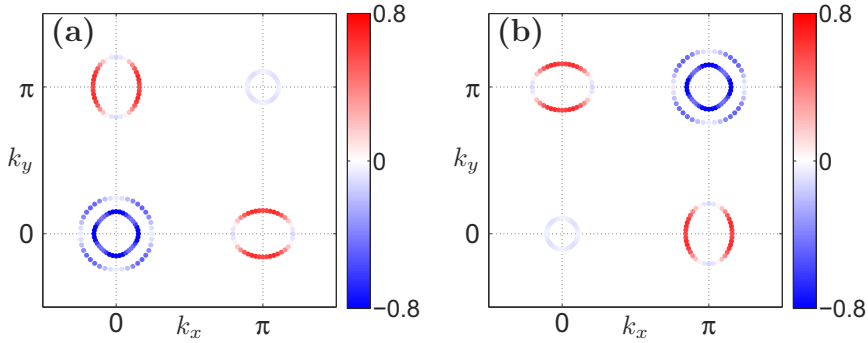

FIG. S4. $\tilde{\Delta}(\mathbf{k})$ calculated at filling $n = 5.95$ for $J = 0$ on Fermi pockets in physical crystal momentum space with odd (a) or even (b) orbital character.